

MODELING OF AN AIRCRAFT CONSTANT SPEED DRIVE

OCTAVIAN GRIGORE-MÛLER¹

Keywords: Constant speed drive; Synchronous generator; Hydraulic unit; Proportional integral derivative controller.

The constant speed constant frequency (CSCF) alternative current electrical power system of an aircraft is based on a constant speed drive (CSD). This type of electrical power system is used on most modern aircraft due to its high inherent reliability and long-life characteristic. This paper presents the design and simulation of an aircraft constant speed drive using the Simscape package of Simulink, a MATLAB program.

1. INTRODUCTION

After World War II, aircraft reliability, flight speed, and capacity increased air transport, especially passenger transport. To attract more passengers to use the airplane, the airlines had to provide comfort and safety above the average used by the other types of transport (maritime, rail, road). Thus, the demand for electricity on board the aircraft increased (see Fig. 1), particularly for the type of high-frequency ac required for radiocommunication and radio navigation systems for safety reasons. As the use of dc on board was limited to 12 kW per channel (due to weight, volume, and energy loss on the distribution electrical network) [1, 2 (pp. 118)], studies and research have been carried out since the '40s to switch to another type of power on board of the aircraft, thus generalizing the use of ac electric power system for high-capacity commercial aircraft [3].

Because of its inherent advantages in weight, size, performance (the highest electrical output per pound per rpm), and efficiency (due to its lowest reactance, the performance under transient load conditions is the best), the salient-pole, synchronous generator with wound poles was chosen like the standard generator of the aircraft electrical power system.

Also, from studies and experiments conducted since the '40s, the frequency of 400 Hz was found to be the near optimum frequency for reduced weight for motors and

generators without a significant increase in wire weight [3].

Thus the 115/200 V ac at 400 Hz frequency was chosen to be the standard of the aircraft electrical power system and has remained the same to this day.

How the generator is a synchronous machine, the frequency of the ac voltage is proportional to the rotational speed of the generator, some methods of converting the variable engine speed in a constant one is needed when dealing with fixed-frequency systems. Thus, was born the first electrical power architecture CSCF.

In a CSCF ac system, primary power is generated by a three-stage wound-field synchronous generator which is driven at a constant speed from a device called CSD. In turn, the CSD is driven by the aircraft engine through a gearbox, at a variable speed, depending on the propulsion power of the engine at different phases of the flight. The CSD, also known as a variable displacement hydraulic transmission, is practically an automatic gearbox which convert the variable speed of the aircraft engine at a constant speed, so that the driven synchronous generator produces current at a constant frequency of 400 Hz within tight limits at the same time.

From historical point of view, the first direct drive hydraulic CSD developed by Sundstrand Aviation (today, Rockwell Avionics, former Hamilton Sundstrand), division of Sundstrand Machine Tool Co. was installed on board the

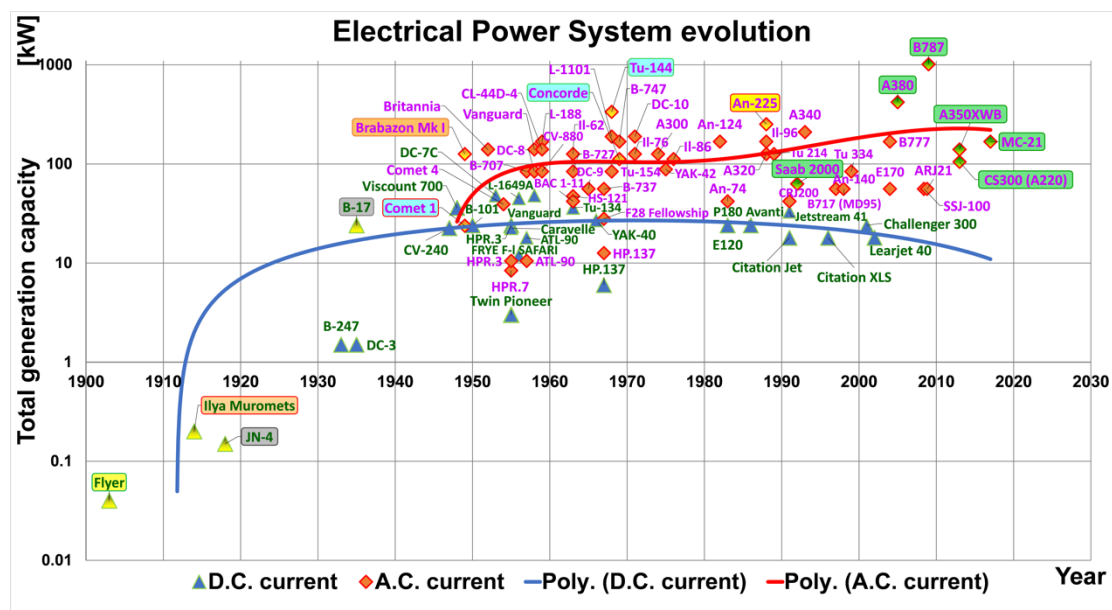


Fig. 1 – The evolution of generation power capacity and type of power for electric power system [4] (pp. 37)

¹ University POLITEHNICA of Bucharest, Faculty of Aerospace Engineering, Department of Aeronautical Systems Engineering and Aeronautical Management, octavian.grigore@gmail.com

will be used. This is composed of a discrete number of pistons N that move in a sinusoidal motion to get the fluid moving. Due to this special design, the fluid flow output of an axial-piston pump is not a smooth straight line. Still, it tends to maintain some of the sinusoidal characteristics of the fluid displacement elements themselves. These are usually called the flow ripple of the pump and are suspected of generating additional vibration and noise [11]. It is assumed that the pump operation begins when one piston is at the zero-reference line, called the 'top dead center (TDC). In this position, the fluid of the piston chamber will begin to be compressed [12].

The VHU hydraulic fluid flow expression [13] (pp. 277), [14] (pp. 33)] is:

$$Q_p = \frac{1}{120\pi} \Omega_p h S N . \quad (1)$$

where: Ω_p is the pump angular velocity;

h – piston stroke;

N – piston number;

S – piston cylinder area.

If R is the distance from the center of the piston shaft to the rotor shaft, then h is:

$$h = 2R \operatorname{tg} \gamma . \quad (2)$$

By introducing this expression, (2), in (1) it will be obtained:

$$Q_p = \frac{SNR \operatorname{tg} \gamma}{60\pi} \Omega_p = C_p \Omega_p \operatorname{tg} \gamma . \quad (3)$$

where $C_p = \frac{SNR}{60\pi}$ is a constant.

From expression (3), to obtain a constant flow at a variable speed, the inclination angle γ of the disc must be changed. If the VHU's flow rate is constant, then the FHU's flow rate will be constant. As the pump and the

flow rate of FHU becomes:

$$Q_m = Q_p - K_p \cdot p_1 = Q_p \left(1 - \frac{K_p \cdot p_1}{Q_p} \right) . \quad (5)$$

where: K_p is the coefficient of losses in the hydraulic circuit of the CSD;

p_1 – high operating pressure of the hydraulic fluid.

The value $\frac{K_p \cdot p_1}{Q_p}$ in relation (5) represents practically

the loss from the circuit and, according to [13] (pp. 279) is a maximum of 5 %.

Due to the pressure delivered by VHU, the FHU pistons will press on the inclined disc with the forces F_1 and respectively F_2 given by [14] (pp. 35):

$$F_1 = p_1 S; \quad F_2 = p_2 S . \quad (6)$$

where p_1 is the high pressure at the inlet of the hydraulic fluid, and p_2 is the low pressure at the fluid outlet from the FHU. According to the first laws of dynamics, the principle of action and reaction, the disk will act on the pistons with the same forces R_1 and respectively R_2 .

These reactions will be decomposed into tangential, R_1'' and R_2'' , and normal R_1' and R_2' respectively, components on the disc's surface. Of these, only the tangential ones give momentum to the FHU rotor axis.

As $p_2 \ll p_1 \Rightarrow R_2'' \ll R_1''$ only the torque created by the force R_1'' acting on the end of the arm x must be evaluated:

$$M_1 = R_1'' \cdot x = R_1' \cdot \frac{D}{2} \sin \varphi = p_2 S \frac{D}{2} \operatorname{tg} \gamma_m \sin \varphi \quad (7)$$

relationship that shows that the motor torque varies

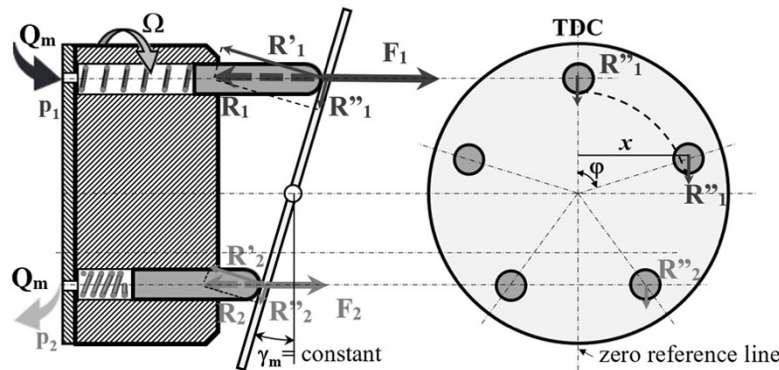


Fig. 4 – Sketch of the forces acting on CSD fixed disk.

hydraulic motor are reversible machines, then the angular velocity of FHU is:

$$Q_m = \frac{SNR \operatorname{tg} \gamma_m}{60\pi} \Omega_m = \frac{1}{C_m} \Omega_m \Rightarrow \Omega_m = C_m Q_m . \quad (4)$$

Due to the imperfect sealing of the hydraulic circuit of the CSD, there are losses given by leakages so that the flow rate of FHU, Q_m is not equal to that of VHU, Q_p . It is assumed that all leakage flows are laminar and have a linear relationship between pressure drop and flow. In this case

sinusoidally with the rotation angle of the FHU rotor.

If the torques produced by all N pistons are added together, the total instantaneous engine torque obtained will be:

$$M_m = \sum_1^N M_i = p_1 S \frac{D}{2} \operatorname{tg} \gamma_m \times \left[\sin \varphi + \sin \left(\varphi + \frac{2\pi}{N} \right) + \sin \left(\varphi + 2 \frac{2\pi}{N} \right) + \dots \right] \quad (8)$$

The torque thus obtained has a pulsating character that can be reduced by choosing a minimum odd number of 7–9

pistons. In this case, the average value of the torque at a rotation angle of 360° is (assuming that in only half a rotation, the pistons are active):

$$M_{med} = NM_{1,med} = \frac{N}{\pi} \int_0^\pi p_1 S \frac{D}{2} \text{tg}\gamma_m \sin \varphi d\varphi = \frac{p_1 NSD \text{tg}\gamma_m}{2\pi} (-\cos \varphi) \Big|_0^\pi = \frac{p_1 NSD \text{tg}\gamma_m}{\pi} \quad (9)$$

By removing p_1 from the relations (4), (5) and (9) results:

$$\Omega_m = C_m(Q_p - K_p \cdot p_1) = C_m \left(Q_p - K_p \frac{M_{med}}{NSD \text{tg}\gamma_m} \right) \quad (10)$$

$$= C_m C_p \Omega_p \text{tg}\gamma - k_1 M_{med} = C \Omega_p \text{tg}\gamma - k_1 M_{med}$$

where: $C = C_m C_p$; $k_1 = \frac{\pi C_m K_p}{NSD \text{tg}\gamma_m}$.

By analyzing the relation (10) it can be concluded that the mechanical characteristic of the CSD is linear with the control angle of the swashplate and slightly falling depending on the value of the average torque. Also, the stiffness k_1 of the characteristic does not depend on the control angle γ .

3. SIMULATION AND RESULTS

To validate the CSD Simulink model was developed a direct drive hydromechanical CSD model used on the B737-300 electrical power generation and distribution system was shown in Fig. 5. The system is composed of the aircraft engine model, the CSD model, the SG model, the generator control unit (GCU) model, that has the role of regulating the voltage of SG with its excitation and the SG frequency through CSD and the last block is the secondary electrical distribution with its loads.

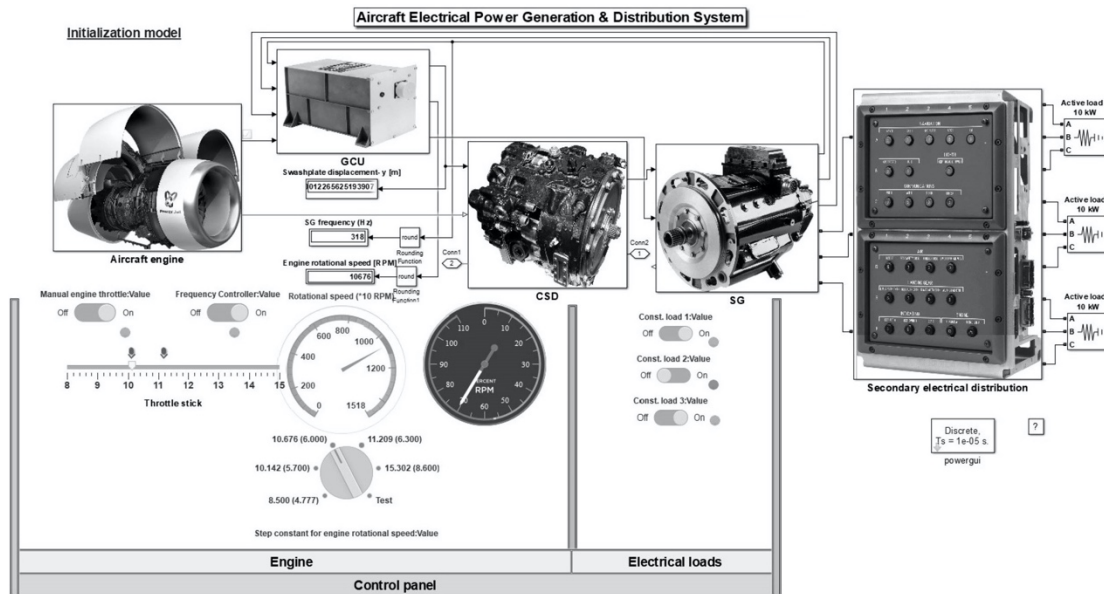


Fig. 5 – Aircraft electrical power generation and distribution system Simulink model.

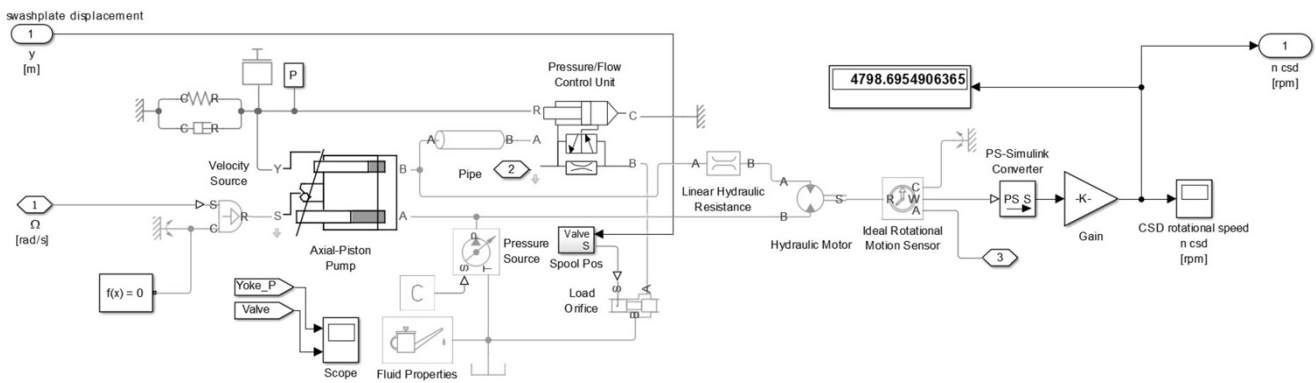


Fig. 6 – CSD Simulink model.

The SG, GCU, and secondary electrical distribution models will be explained in a later paper. In that case, the CSD Simulink model is shown in Fig. 6. The CSD model consists of the updated Simulink axial-piston pump model "Hydraulic Axial-Piston Pump with Load-Sensing and Pressure-Limiting Control" [15] to nine pistons, a hydraulic motor with a linear hydraulic resistance and a lookup table

with the values of the swashplate displacement included in the generator control unit (GCU) block.

The simulation of the CSD, the whole model of the electrical power generation and distribution system of the B737-300 aircraft, is performed in Simulink / MATLAB v.9.0. The simulation parameters are listed in Fig. 7, according to [16–19].

MATLAB Workspace		Page 1
Mar 20, 2022		4:40:11 PM
Name	Value	
act_arm	0.0320	
actuator_init_pos	1.0000e-03	
actuator_stroke	0.0080	
carryover_angle	0.1222	
hydraulic_fluid	'MIL-F-87257'	
number_pistons	9	
orifice_diameter	1.0000e-03	
piston_area	1.0710e-04	
piston_stroke	0.0220	
pitch_radius	0.0058	
Tfuse	0.1000	
tr_slot_angle	0.0347	
tr_slot_area	1.0000e-06	
Ts	1.0000e-05	
viscous_friction_coefficient	14	

Fig. 7 – The simulation parameters for Simulink model

The CFM-56-3-B1 engine rotational speed (for high-pressure rotor – N2) of B737-300 aircraft, which drives the CSD according to [20] (pp. 7), [21] (pp. 8) is: minimum in icing condition – 8500 rpm and maximum – 15183 rpm.

How according to [21] (pp. 6) the gear ratio to drive the aircraft electrical generator is 0.562 CW (clockwise), it means that the CSD input rotational speed is:

$$\begin{aligned} \text{at minimum: } & 8500 \times 0.562 = 4777 \text{ rpm;} \\ \text{at maximum: } & 15183 \times 0.562 = 8533 \text{ rpm.} \end{aligned} \quad (11)$$

From the CSD manufacturer specification, the CSD input rotational speed is between 4300 rpm and 8600 rpm, and the output rotational speed (that is, the speed which drives the

SG) is 6000 rpm. In this case, in simulation, it was chosen as the input rotational speed for CSD, the values listed in Table 1. These values can also be seen on the knob in Fig. 5.

Table 1

Rotational speed and swash plate displacement for model simulation

Nr.crt.	Aircraft engine rotational speed [rpm]	CSD rotational speed [rpm]	Swash plate displacement [m]	Swash plate angle γ [°]
(1)	(2)	(3) = (2)×0.562	(4)	Arctan [(4)/0.032]
1.	7651	4300	-0.001326682	-2.37
2.	10142	5700	-0.001089228	-1.95
3.	10676	6000	-0.001036527	-1.85
4.	11209	6300	-0.000983082	-1.76
5.	15302	8600	-0.000541868	-0.97
6	16991	9549	-0.000338409	-0.60
7	21352	12000	0.000278839	0.50

As the speed limits of the CSD have been determined, the next step is to find out the displacement of the swash plate to obtain these rotational speeds. The order of magnitude of the initial value was approximated from the patents of the manufacturer Hamilton Sundstrand [16–18].

From relation (2), respectively (10), it can be observed that the displacement of the swashplate is proportional to the rotational speed using the γ angle, in which case a linear controller can be developed with the help of block "n-D Lookup Table" from Simulink based on the linear interpolation operation.

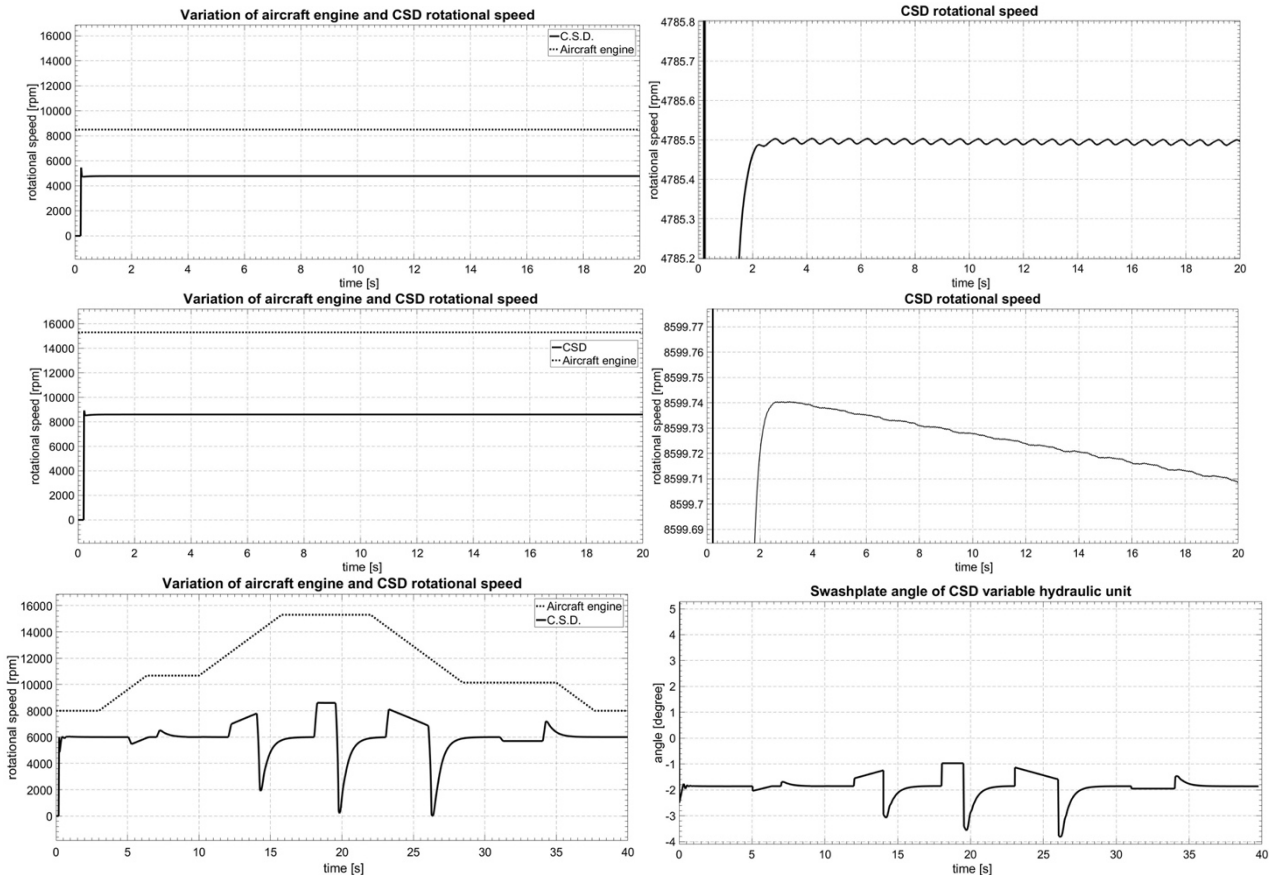


Fig. 8 – Characteristics of the aircraft engine and CSD.

Because the characteristic of the "hydraulic motor" block in Simulink and Simulink axial-piston pump model [15] are ideal for simulating the inherent hydraulic leakages that occur in the

two hydraulic machines and the corresponding hydraulic circuit (pipes) and obtaining the slightly falling linear mechanical characteristic of the CSD (10), a linear hydraulic

resistance was introduced before the hydraulic motor block. To obtain a constant rotational speed at the output of the CSD to drive the SG, its rotational speed is adjusted with a proportional integral derivative controller (PID) from the discrete library of the Simulink, which has been included in the GCU block. Since one of the PID inputs is the frequency of the CSD-driven SG, a generator not covered by this article, it will be briefly mentioned that the PID has been adjusted so that the order of magnitude of its output matches the values of swashplate displacement in the Table. 1.

Thus, Fig. 8 shows the mechanical characteristics of the CSD for the drive rotational speeds determined and specified in Fig. 5 and Table 1. From there, it can observe the slightly falling linear mechanical characteristics of the CSD for 4777 rpm (the minimum CFM-56-3-B1 engine rotational speed (11)) and 8600 rpm, the maximum allowed rotational speed for CSD. This fall increases with the increase of the CSD rotational speed. It can also see the pulsating character of these characteristics, where the signal's frequency increases with CSD input rotational speed. The last two images in Fig. 8 show the CSD operation by the aircraft engine with a variable speed, as is usually the case in a standard flight mission.

The manufacturer's recommended CSD test data was used to generate the mechanical aircraft engine profile. Among these, it reminds: the testing of the CSD will be done between 3000 and 13500 rpm, with acceleration and deceleration of the drive motor between 50 and 800 rpm/s; rotational speed must stabilize within 3 to 6 s, with a maximum error of $\pm 2\%$.

The image on the bottom right shows the CSD command via the swashplate angle γ . Also, at seconds 5, 9, 12, 18, 23, and 31, the PID controller was disconnected for a few seconds, which can be seen in the CSD characteristic's overshoot.

From the last two images, the proportionality of the CSD control signal with its rotational speed should be noted, a relationship already established by eq. (10).

4. CONCLUSIONS

The research on civil aircraft's CSD has lasted more than 75 years. Due to recent developments in computer science, hydraulics, materials, processes technology, sensors, and signal acquisition is a fully developed technology. This paper presents an overview of the description and a simulation with the Simulink/Matlab of the CSD used in most modern civil aircraft. Some of the challenges, such as the values of the CSD components and the restricted data of its testing mechanical characteristic, have conducted new requirements for the simulation of the other two blocks, SG and GCU.

Received on 28 March 2022

REFERENCES

1. T. Simms, *Aircraft Electrical Generating Systems: A Review of Recent Developments and Design Trends*, Aircraft Engineering and Aerospace Technology, **33**, 12, pp. 344–350 (1961).
2. *Aviation Electrician's Mate 3&2*, NAVPERS 10348-B, Bureau of Naval Personnel, United States Navy Training Publications Center, Memphis, Tennessee, 1965, p. 118.
3. A.K. Hyder, *A Century of Aerospace Electrical Power Technology*, Journal of Propulsion and Power, **19**, 6, pp. 1155–1179 (2003).
4. O. Grigore-Müller, *Aircraft electrical power system. Analysis and design*, (in Romanian) Matrix ROM, Bucharest Romania, p. 37 (2021).
5. Tamara Thiessen, *40% Less Flights Worldwide: This Is What's Happening with Air Travel*, Forbes, Apr.1 (2020).
6. A. Doyle, *Tracking the in-storage fleet and utilization in a time of uncertainty*, Cirium, 29.05 (2020).
7. *ODs-June-2020-Airbus-Commercial-Aircraft*, www.airbus.com/aircraft/market/orders-deliveries.html#file.
8. ****Orders & Deliveries, Revenue Recognition Accounting Standard ASC 606 Information, Orders through 06/30/2020*, www.boeing.com/commercial/#/orders-deliveries
9. ****Hamilton Sundstrand Brochure*, Hamilton Sundstrand, A United Technologies Company, 080397.indd, 12 Nov. 2008.
10. C.J. Gantzer, *Combined fluid and mechanical drive*, US3365981A patent, 30.01 (1968).
11. N.D. Manring, *The Discharge Flow Ripple of an Axial-Piston Swash-Plate Type Hydrostatic Pump*, Journal of Dynamic Systems, Measurement and Control, **122**, 2, pp. 263–268 (2000).
12. G. Changbin, J. Zongxia, H. Shouzhan, *Theoretical study of flow ripple for an aviation axial-piston pump with damping holes in the valve plate*, Chinese Journal of Aeronautics, **27**, 1, pp. 169–181 (2014).
13. I. Aron, V. Păun, *Echipamentul electric al aeronavelor*, (in Romanian) Ed. Didactică și Pedagogică, București, 1980, p. 277.
14. D. Dinu, *Mașini hidraulice și pneumatice utilizate în domeniul naval*, Ed. Nautica, Constanța, România, 2019, p. 33.
15. *Hydraulic Axial-Piston Pump with Load-Sensing and Pressure-Limiting Control*, MathWorks Documentation, <https://www.mathworks.com/help/physmod/hydro/ug/hydraulic-axial-piston-pump-with-load-sensing-and-pressure-limiting-control.html>.
16. K.H. Campbell, G.C. Lemmers Jr., M.J. Franklin, *Cylinder block assembly for hydraulic unit*, US20160273531A1 patent, 22.09 (2016).
17. D.R. Hochstetler, T.A. Martin, D.C. Johnson, G.C. Lemmers Jr., *Hydraulic unit cylinder block for integrated drive generator*, US10539213B2 patent, 21.01 (2020).
18. D.R. Hochstetler, T.A. Martin, D.C. Johnson, G.C. Lemmers Jr., *Variable wobbler plate for integrated drive generator*, US10707792B2 patent, 7.07 (2020).
19. *Shop talk: Change in hydraulic fluid*, Newsletter, Onboard systems international, 30/09/2017, <https://www.onboardsystems.com/news/newsletter/154>.
20. *Boeing 737 Type-certificate data sheet*, EASA TCDS No.: IM.A.120, 25, European Union Aviation Safety Agency, 2022, p. 7.
21. *CFM56-2 & CFM56-3 series engines Type-certificate data sheet*, EASA TCDS No.: E.066, 1, European Union Aviation Safety Agency, p. 6, 2008.